

Accepted Manuscript

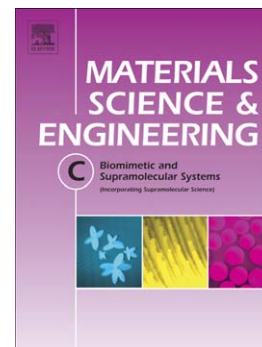
Effect of biomimetic 3D environment of an injectable polymeric scaffold on MG-63 osteoblastic-cell response

Shalini Verma, Neeraj Kumar

PII: S0928-4931(10)00140-2
DOI: doi: [10.1016/j.msec.2010.06.005](https://doi.org/10.1016/j.msec.2010.06.005)
Reference: MSC 2871

To appear in: *Materials Science & Engineering C*

Received date: 29 December 2009
Revised date: 7 May 2010
Accepted date: 8 June 2010



Please cite this article as: Shalini Verma, Neeraj Kumar, Effect of biomimetic 3D environment of an injectable polymeric scaffold on MG-63 osteoblastic-cell response, *Materials Science & Engineering C* (2010), doi: [10.1016/j.msec.2010.06.005](https://doi.org/10.1016/j.msec.2010.06.005)

This is a PDF file of an unedited manuscript that has been accepted for publication. As a service to our customers we are providing this early version of the manuscript. The manuscript will undergo copyediting, typesetting, and review of the resulting proof before it is published in its final form. Please note that during the production process errors may be discovered which could affect the content, and all legal disclaimers that apply to the journal pertain.

Effect of biomimetic 3D environment of an injectable polymeric scaffold on MG-63 osteoblastic-cell response

Shalini Verma and Neeraj Kumar*

Department of Pharmaceutics, National Institute of Pharmaceutical Education and Research (NIPER),
Sector 67, S. A. S. Nagar (Mohali)-160062, INDIA.

Phone: +91-172-2292057; Fax: +91-172-2214692; E.mail: <neeraj@niper.ac.in>

*Corresponding author

Abstract

Solid PLGA microspheres were fabricated and characterized in terms of their *in vitro* degradation behaviour. Microsphere scaffolds were then modified covalently by P-15 (GTPGPQGIAGQRGVV) to obtain a 3D bioactive collagen surrogate matrix for bone filling applications. These scaffolds were characterized for surface topography, hydrophilicity and evaluated for their effect on osteoblastic activity of MG-63 cell line *vis-a-vis* 2D monolayer culture.

AFM and contact angle experiments indicated enhanced nano-level roughness and hydrophilicity on P-15 modification. Modified scaffolds showed enhanced cell attachment, proliferation, extracellular matrix formation, mineralization and collagen type-I expression when compared to unmodified microspheres, prerequisite for bone filling applications. On long term *in vitro* cell culture, however, decreased cell viability was observed which may be attributed to the acidic microenvironment generated due to polymer degradation and reduction in nutrient diffusion through the copious ECM formed in 3D scaffolds. Though a higher cell count could be obtained in 2D monolayer cell culture, it was overshadowed by weak cell attachment, poor phenotypic characteristics, decreased cell viability and low mineralization levels, over 28 day cell culture studies.

Results indicate that P-15 modified microsphere scaffolds may provide a natural, biomimetic 3D environment and may be successfully exploited for non-invasive bone filling applications.

Keywords: Biomimetic 3D scaffold; MG-63; degradation; P-15; PLGA; surface modification; 2D Vs 3D culture

1. Introduction

One of the major challenges of bone-tissue engineering is to design a matrix that is capable of mimicking the natural properties of bone while providing a temporary scaffold for tissue regeneration. Initially, materials intended for implantation were designed to be ‘bio-inert’. However, the current focus has shifted towards the design of deliberately ‘bioactive’ materials that integrate with biological molecules or cells and regenerate tissues [1, 2]. In the case of bone filling applications, materials should preferably be both osteoconductive (support bone growth and encourage the in-growth of surrounding bone) and osteoinductive (capable of promoting the differentiation of progenitor cells down an osteoblastic lineage), as well as capable of osseointegration (integrate into surrounding bone).

Osteoconductive matrices are fabricated from biodegradable materials of natural origin and most commonly from synthetic polymers such as poly (lactic-co-glycolic) acid (PLGA). The matrix used as a scaffold should satisfy certain requirements. They should be designed to allow diffusion of nutrients to the transplanted cells and guide cell organization, attachment, migration and differentiation. They should also be biodegradable and bioresorbable. Literature reports support the fact that changes in scaffold surface chemistry and topography alter cellular activity [3, 4]. Therefore, surface may need to be characterized or even altered to facilitate bone tissue regeneration. Surface modification of biomaterials with bioactive molecules such as a native long chain of extracellular matrix (ECM) proteins (e.g. fibronectin, vitronectin, and laminin) as well as short peptide sequences derived from intact ECM proteins (e.g. RGD found in fibronectin, collagen, and vitronectin; REDV found in fibronectin; GTPGPQGIAGQRGVV (P-15) found in collagen) is an attractive approach to develop biomimetic niches which interact bio-molecularly with the cells to control their function, guiding the spatially and temporally complex multicellular processes, and facilitating tissue regeneration [5-9]. The use of short cell-binding peptides is however advantageous over long-chain native ECM proteins as they are flexible, experience minimal steric effect, have usually lower immunogenicity, can be easily synthesized and purified at relatively low costs and are more stable than large ECM proteins during the surface modification and sterilization processes [10].

Though a number of scaffold types have been explored for tissue engineering and regeneration applications, many groups have recently demonstrated the potential of

polymeric microsphere scaffolds/microcarriers as transplantation matrices [11-15]. Our group has also previously reported solid PLCL microspheres for growth and proliferation of epithelial and myoblast cells [16]. Microcarriers provide a three-dimensional (3D) environment for cell growth and at the same time, offer an attractive alternative to avoid the limitations of current *ex vivo* cell expansion methods for clinical-scale production (2D culture plates) [17]. Biodegradable microsphere scaffolds can potentially be used *in vitro* as a mouldable and injectable scaffold for cellular delivery [18, 19]. Moreover, one can also load specific growth factors or ECM proteins to promote cell proliferation and differentiation on these scaffolds. With the growing popularity of non-invasive arthroscopic procedures, injectable scaffolds are particularly promising for bone regeneration, especially for treating irregularly shaped defects in applications such as vertebroplasty, unicameral bone cysts, tumour resection surgeries, osteoporotic bone fractures and other clinical conditions requiring bone defect filling.

In the light of above discussion, the present study aimed at modifying the hydrophobic surface of PLGA microsphere scaffolds with a biomimetic cell adhesion peptide; P-15 (GTPGPQGIAGQRGVV) (MediScient, USA), a synthetic analogue of cell-binding domain of $\alpha 1(I)$ chain sequence of human type I collagen, so as to impart cell recognition signals for development of an osteoinductive, injectable bone filler. We evaluated P-15 modified PLGA microsphere scaffolds (P-15 MS) for attachment and proliferation of osteoblast-like cell line (MG-63). The response of cells to 2D monolayer and 3D microsphere scaffold environment was investigated during 28 days by *in vitro* cell culture studies. The *in vitro* degradation of the microsphere scaffolds was studied since it has a profound effect on cell viability and growth and also on *in vivo* fate of the scaffold after implantation. An attempt has been made to correlate the degradation pattern of 3D solid microspheres to their *in vitro* cell culture behaviour.

2. Materials and methods

2.1. Microsphere scaffold fabrication

Microspheres were prepared by solvent evaporation method. PLGA 50:50 (I.V. 0.55-0.75 dL/g, DURECT Corporation) solution in dichloromethane was added drop wise into poly vinyl alcohol solution (PVA, 30000-70000 Da, Sigma) while stirring to form an o/w emulsion. After evaporation of organic solvent (4h), microspheres were recovered, washed and dried at room temperature (RT) under vacuum. Microsphere size was calculated using IMT i-Solution imaging software (Version 7.5).

2.2. Surface modification of microspheres for induction of biomimetic features

The biomimetic surface modification was performed by covalently coupling P-15 peptide on to microsphere surface by carbodiimide coupling procedure. Free COOH groups on the surface of microspheres were determined by simple acid-base titration in aqueous medium [20]. The molar ratio of free COOH: N-hydroxy succinimide (NHS) (Sigma): (N-(3-Dimethylaminopropyl)-N'-ethyl carbodiimide hydrochloride (EDC) (Sigma) was kept as 1:1.5:2 for the reaction. The COOH groups were first activated in coupling solution (containing NHS and EDC) for 30 min after which P-15 was added to reaction mixture (final concentration: 100 µg/ml). The reaction was performed at pH 5.5 for 24 h with slight shaking at RT. After completion of the reaction, the microspheres were washed several times with distilled water, dried under vacuum at RT and stored at -20°C. P-15, being an aliphatic peptide, lacks UV absorbance. Hence, spectrofluorimetric derivatization of hydrolyzed P-15, using o-phthalaldehyde-N-acetyl cysteine (OPA-NAC), was developed and used for estimation of coupling efficiency. Reaction of OPA with SH-group containing molecules such as NAC and primary amino groups (amino acids) results in a 1-alkylthio-2-alkyl-substituted isoindole [21]. The resulting isoindole derivatives reveal a fluorescence excitation (λ_{ex} 345 nm) and emission (λ_{em} 450 nm) spectra. Coupling efficiency was calculated indirectly by depletion method, where the difference between initial (Total amount of P-15 initially added into the reaction medium) and final (Total amount of P-15 remaining in the reaction medium and obtained in the washings, after 24h) concentration of P-15 in the reaction mixture gave an indirect measure of coupling efficiency. Serial dilutions of known concentrations of P-15 spiked with EDC and NHS were used as standards for preparation of calibration curve.

2.3. Characterization of P-15 modified scaffold

2.3.1. Surface topography

Atomic force microscopy (AFM) was performed to study the effect of P-15 surface modification on surface roughness and topography of microsphere scaffolds. Five scans ($3 \times 3 \mu\text{m}$) were analyzed for both unmodified (MS) and P-15 modified microsphere (P-15 MS) scaffolds using BioScope II microscope (Veeco Instruments Inc.). Images of the surfaces were obtained in tapping mode using Rotating tipped Etched Silicon Probe (RTESP) Phosphorous (n) doped cantilevers (Veeco Instruments). The topography of the surface and average roughness (Ra) were obtained using the built-in software (NanoScope 7.10 image processing software). Height phase images were recorded with the maximum available number of pixels (512×512).

2.3.2. Contact angle measurement

The change in hydrophobicity of polymeric surface after P-15 modification was studied by contact angle measurements using sessile drop method, using a $5 \mu\text{l}$ water droplet in a telescopic goniometer (FTA 1000 Drop Shape Instrument, U.S.A.) until the largest contact angle was achieved without increasing the solid/liquid interfacial area. A smooth and uniform surface is a prerequisite for reliable contact angle determination. This was, however, impossible for microsphere scaffolds due to their size and shape. Hence, films of PLGA were fabricated on glass slides and modified with P-15, as mentioned in section 2.2. Films thus obtained were used for contact angle determination ($n=9$) [22].

2.4. Degradation studies

The *in vitro* degradation behaviour of microsphere scaffolds was assessed by placing 20 mg MS in 1.0 ml of phosphate buffer (100 mM, pH 7.4) with sodium azide (0.02% w/v) as a bactericide. The samples were kept in a shaking water bath maintained at 37°C , 100 cycles/min during the study period. At various time points, over a span of 60 days, the pH of degradation medium was measured as an indicative of extent of degradation. MS were weighed after removal of degradation medium to get the wet weight and then were vacuum dried to a constant weight at a temperature below 40°C . The percentage mass loss and degree of hydration were calculated as per equation (1) and (2) respectively.

$$\% \text{ Mass loss} = (W_o - W_d) / W_o \times 100 \dots (1)$$

$$\text{Degree of hydration} = (W_w - W_d) / W_d \dots (2)$$

Where, W_o = Original weight of MS; W_w = Wet weight of MS; W_d = Dry weight of MS after vacuum drying to constant weight.

At predetermined intervals, molecular weight changes were tracked by GPC using Styragel[®] HR3 & HR4 column (7.8×300 mm) with chloroform as solvent at 30°C and mono-disperse polystyrene as calibration standards. The copolymer composition was determined by ¹H NMR where the samples dissolved in a small quantity of deuteriated chloroform (CDCl₃) were analyzed by Bruker (Avane DPX 300) in the chemical shift range (δ) of 0-13 ppm using tetramethylsilane as a reference standard. Changes in surface morphology, during scaffold degradation, were studied by scanning electron microscopy (SEM). Dried MS were mounted on the stub, gold sputter coated (30 s) and observed using S-3400N scanning electron microscope (Hitachi, Japan).

2.5. *In vitro* cell culture studies

Osteoblast-like cells (MG-63) (NCCS, Pune) were used for *in vitro* cell culture studies. The cells were cultured in Dulbecco's Modified Eagle Medium (DMEM) (Life Technologies, India) supplemented with 10% foetal bovine serum (FBS) (Life Technologies, India) and 1% antibiotic (Penicillin (100 IU/ml), streptomycin (100 μ g/ml) and amphotericin B (2.5 mg/ml) (Calbiochem, Germany), in 5% CO₂ at 37°C. Scaffold sterilization was done by placing the samples (MS and P-15 MS) in absolute ethanol for 2 h followed by UV exposure (30 min). The sterilized microspheres (22 mg/well) were then transferred to Costar[®] Ultra low cluster 24 well plates (Corning, Catalogue #3473) and seeded with 0.2 million cells/well for 3D cell culture studies. For 2D monolayer cell culture studies, 40,000 cells were directly seeded on each well of Costar[®] tissue culture treated 24 well plate (Corning, Catalogue #3526). During the first 24 h, cells were cultured in absence of FBS, to eliminate the effect of serum proteins on initial cell attachment. Later, the medium was replaced with DMEM containing 1% antibiotic and 10% FBS.

2.5.1. Cell attachment and proliferation studies

Cell adhesion was determined on 2D monolayer culture, MS and P-15 MS after 24h of cell seeding. Briefly, the medium was aspirated; samples were washed by PBS to remove the unattached cells and the attached cell count was determined by trypsinization followed by trypan blue staining. MTT assay was used to study whether P-15 modification on 3D microsphere surface had an effect on the long term cell viability and proliferation of osteoblast-like MG-63 cells on microsphere scaffolds, over a period of 28 days. 2D monolayer culture was also performed and compared with the 3D scaffolds (MS as well as P-15 MS).

2.5.2. Cell morphology

The morphology of cells growing on 2D monolayer culture and 3D scaffolds was studied using optical microscopy. Such visualization helped in determining the pattern of cell growth and cellular arrangement of cell-scaffold constructs.

The morphology of cell-scaffold constructs was further explored by SEM, where the constructs were gently washed with PBS followed by an overnight fixation using 2.5% glutaraldehyde solution buffered with 0.2 M cacodylate buffer (pH 7.4), at RT. After this, cells were dehydrated in ethanol/distilled water mixture from 50% to 100% ethanol in steps of 10% for 10 min each. Samples were then air-dried, gold sputter coated (30 s) and observed using S-3400N scanning electron microscope (Hitachi, Japan).

2.5.3. Cytoskeleton organization

The cytoskeleton arrangement, of cells cultured on MS and P-15 MS, was observed by fluorescent labelling of actin filaments with Rhodamine 110 phalloidin (Biotium Inc., USA), as per manufacturer's instructions followed by imaging by confocal microscopy (Olympus Fluoview FV 1000, Japan). The images were collected as z-sections and multiple sections were projected onto one plane for presentation.

2.5.4. Protein estimation

Generation of matrix proteins with required quantity and quality is valuable evidence towards the formation of functional tissues *via* tissue engineering. Hence, Bradford colorimetric assay was used to determine the protein content in both 2D and 3D scaffolds as a quantitative measure of matrix protein production, using bovine serum albumin (BSA) as a standard.

2.5.5. Cell differentiation studies

Alkaline phosphatase (ALP) activity and osteopontin (OPN) content were determined as a marker of cell differentiation on day 21. For this, cell culture medium was aspirated and samples were rinsed with PBS. In case of 2D monolayer culture, cells were harvested by trypsinization. Cells obtained in 2D monolayer culture and microsphere-cell constructs (MS and P-15 MS) were placed in 500 μ l lysis buffer containing 50mM Tris (pH 6.8), 0.1% triton-X 100 and 2mM magnesium chloride and sonicated for 3×10 s at 60 Amp in ice. ALP activity was determined in the cell lysate using Autozyme ALP kinetic kit (Accurex Biomedical Pvt. Ltd.) as per manufacturer's instructions. For OPN content determination, rat OPN ELISA kit (# CSB-E08393 r, Cusabio Biotech Co. Ltd.) was used. The effect of P-15 modification on the quality of ECM formed was characterized in terms of matrix mineralization and collagen Type-I expression. High levels of mineralization and collagen

expression are an indication of the success of a scaffold in bone tissue engineering applications since Type-I collagen is the main element of the mineralized ECM in bone. Mineralization of formed scaffold-cell construct was determined by alizarin red staining.

Phenotypical characterization of ECM was carried out by immunohistochemical evaluation of Type-I collagen using a labelled streptavidin biotin (LSAB) method. Briefly, antigen retrieval was done on formaldehyde fixed samples by the Proteinase K method. Residual enzymatic activity was removed by washing in PBS followed by treatment with 3% H₂O₂ solution for 10 min to reduce endogenous peroxidase activity. Non-specific staining was blocked with 10% FBS for 30 min. Samples were incubated with a monoclonal anti-collagen Type-I clone COL-1 (Sigma, catalogue # C2456) (1:2000 dilution in PBS) for 1 h, washed, and incubated with a Immunopure® Biotin conjugated secondary antibody (Thermo Scientific, USA, #31807) (1:500 dilution in PBS) for 30 min. Samples were washed and subjected to Streptavidin-peroxidase Polymer, Ultrasensitive (Sigma, USA) (1:500 dilution in PBS), for 15 min, washed, and exposed to diaminobenzidine (Sigma, USA) for 15 min followed by counterstaining with hematoxylin & eosin (Qualigens Fine Chemicals, India). Digital photomicrographs were obtained using a TC5500 microscope equipped with an Infinity-1 camera (Meiji Techno, Japan).

2.6. Statistical analysis

All sample values were expressed as mean \pm standard deviation (SD), with n=3 and the data were analyzed using SigmaStat Version 3.5. Statistically significant values were defined as $p < 0.050$ based on one-way analysis of variance (ANOVA) followed by Student-Newman-Keuls test.

3. Results

3.1. *Microsphere scaffold fabrication and biomimetic modification*

Microspheres were fabricated in the size range: $102.74 \pm 12.38 \mu\text{m}$, with a yield greater than 90%. The parameters used for microsphere fabrication were: organic to aqueous phase ratio: 1:50; stirring rate: 450 rpm; polymer concentration: 50mg/ml; and PVA concentration: 0.5% w/v.

For biomimetic modification, the number of acid functionalities (acid number) were firstly determined to calculate amount of free -COOH groups on microsphere surface. Acid number was found to be 7.475 ($\approx 0.133 \text{ mM}$ surface free COOH/g) and was used for calculating the amount of coupling reagents required for surface modification of microspheres. P-15 coupling was found to be $94.6 \mu\text{g}$ per gram of microsphere scaffolds.

3.2. *P-15 modified scaffold characterization*

3.2.1. Surface topography

Surface roughness has been reported to have an effect on cell spreading and growth [23, 24]. In general, surface roughness increases initial cell attachment, migration, and ECM production. The effect of P-15 coupling on surface characteristics of microsphere scaffolds was studied by AFM (Figure 1). P-15 coupling led to the formation of undulations and ridges on microsphere surface. The simplest and most common method used for the observation of changes in surface topography is Image Ra. This roughness calculation is based on finding arithmetic average of absolute values of surface height deviations measured from the mean plane. It was found that the Ra values increased from $5.33 \pm 0.45 \text{ nm}$ to $200.20 \pm 13.37 \text{ nm}$ after covalent surface modification of PLGA microsphere surface with P-15 peptide. This increase in nano-scale roughness is expected to result in increased cell attachment and improved cytoskeletal arrangement and cell orientation.

3.2.2. Contact angle measurement

The contact angle of a given surface is an indicative of its hydrophilicity. Lower the contact angle, higher is the hydrophilicity. The aim of this study was to investigate the effect of P-15 modification on hydrophilicity of polymeric surface. It was found that the surface modification of PLGA films with P-15 peptide resulted in a reduction of the contact angle from $65.93 \pm 1.09^\circ$ to $57.21 \pm 2.15^\circ$, demonstrating an increased hydrophilicity and wettability. The results indicated that P-15 modification provides a more favourable environment for cell attachment and growth.

3.3. Degradation studies

PLGA degrades by bulk erosion as water penetrates into the polymer matrix and leads to subsequent hydrolytic cleavage of ester bonds [25]. The hydrolysis of ester bonds can be catalyzed by free carboxyl end groups within the same molecule (intramolecular catalysis) or by other acidic moieties such as lactic and glycolic acids; the degradation products of PLGA that accumulate within the hydrated microsphere (intermolecular catalysis). These degradation by-products also result in generation of an acidic microenvironment in apposition to the growing cells, which is detrimental to the cell growth. The factors that influence the chemical degradation of PLGA include polymer molecular weight, ratio of lactic to glycolic acid in the co-polymer, environmental temperature, pH, and geometry of the scaffold [26].

Degradation of polymeric scaffold led to molecular weight loss due to conversion of polymer chains into small oligomers and finally soluble lactic and glycolic acids. Weight average molecular weight (M_w) of MS decreased exponentially with degradation time throughout the degradation period (Figure 2A). Apparent degradation rate constant (K_{Mw}) and degradation half life ($t_{1/2Mw}$) were calculated to be 0.032 week^{-1} and 9.44 weeks, respectively. A sharp weight loss was observed after an initial lag time of about 20 days, with almost 40% weight loss in 30 days (Figure 2A). The degree of hydration was also investigated as a measure of polymer degradation. MS exhibited a high degree of hydration and swelling due to the presence of free -COOH groups in the polymer (Figure 2B). As hydration occurred, microspheres swelled and increased in size due to water ingress. After about 20 days of degradation, the extent of degradation exceeded the hydration resulting in a steep fall in the degree of hydration (Figure 2B). At the same time, pH of the degradation medium fell (7.4 to 3.9 in about 27 days) and then reached a plateau indicating that PLGA microspheres were completely degraded. A shift was observed in the copolymer composition from 50 mol% at day 0 to 70 mol% at 42 day as preferential cleavage occurred at the glycolic-glycolic and glycolic-lactic bonds thereby causing a faster release of glycolic acid. The initially smooth and spherical microspheres also showed visible signs of bulk degradation as indicated by SEM results (Figure 2C-F).

3.4. *In vitro* cell culture studies

3.4.1. Cell adhesion, viability and proliferation studies

Cell–matrix/cell–scaffold interactions are the basis of initial cell attachment and also influence the cell phenotype and functions. During the first 24 h of the study, FBS was excluded from cell culture medium so as to avoid the effect of serum proteins on initial cell

attachment. P-15 MS showed significantly higher cell attachment efficiency than MS (Figure 3). This may be attributed to the ability of P-15 to enhance cell adhesion and to reduce apoptosis levels in serum-free conditions [27]. A significantly higher cell count was observed in P-15 MS than on MS due to enhanced cell attachment and biomimetic surface environment provided by P-15 peptide until day 21 (Figure 4A). For both 2D plate and 3D microsphere scaffolds, cell viability and corresponding cell count increased till 14 day and later decreased. The cell viability remained significantly higher on 2D plate than on both MS and P-15 MS on 7th, 14th and 21st day, as multiple layers of cellular clusters were formed in 2D plate. However, on 28th day, cell attachment on plate surface was completely lost and led to detachment of almost all cells in the form of loose clusters. Although cell viability declined during the later phase of study, cell attachment to scaffolds was maintained in 3D scaffolds until the end of the study, unlike in 2D monolayer culture, indicating the beneficial effect of 3D environment in maintaining the cell growth.

3.4.2. Morphology

Cell morphology and cellular arrangement on 2D monolayer culture plates as well as on 3D scaffold-cell constructs, was studied using optical microscopy and SEM. In 2D cultures, a uniform layer of flattened cells with very few rounded cells could be seen on 7th day (Figure 5A2). As the study progressed, clusters of rounded dead cells became visible which later detached leaving empty spaces (Figure 5A3, A5). These observations were consistent in all other supporting experiments. In case of 3D scaffolds, cells were visible on the periphery of microsphere scaffolds, alone or in clusters, on 1st day (Figure 5B1, C1). In due course, uniform layers of flattened cells were formed on the microsphere surface which further led to ECM formation and cellular bridges across 3D microsphere scaffolds. Cell attachment was maintained in 3D scaffolds during the complete course of study suggesting higher strength of cell attachment and focal contacts on 3D scaffolds.

P-15 MS showed significantly higher level of ECM production resulting in formation of remarkably well organized, highly arranged, interconnected 3D colonies, much earlier than the MS (Figure 5C3, B5). Signs of bulk degradation were visible in both MS and P-15 MS leading to microsphere hydration and swelling, as early as 7 days of cell culture. When degradation studies were performed in absence of cells in PBS, maximum hydration and swelling were observed after 20 days. In presence of cells, however, a significant hydration and swelling was visible on 7th day. This may be due to increased rate of enzymatic degradation of polymer in presence of cells. The pores generated due to bulk degradation of

3D scaffolds were later replaced by cells and ECM, thus forming a continuous sheet of tissue-like construct (Figure 5B5, C5).

SEM micrographs of P-15 MS showed higher interconnectivity and cellular bridging in comparison to MS, on 7th day, in concordance with optical micrographs. At the same time, a thicker layer of cells forming interconnected bridges could be observed in biomimetic P-15 MS (Figure 6B). These bridges were responsible for formation of uniformly arranged 3D colonies in P-15 MS, in early stages of study. Such interconnectivity and cellular bridging was absent in MS on 7th day (Figure 6A).

3.4.3. Cytoskeleton arrangement

The generation of mechanical forces by the cellular cytoskeleton plays a critical role in the organization of ECM and of cellular colonies. The anchorage of the cytoskeleton to a substrate is essential for cellular tractional processes. Since P-15 is believed to engage the cytoskeleton, cytoskeleton arrangement of cells growing on 2D and on 3D MS and P-15 MS was studied using fluorescent labelling of cells with Rhodamine 110 phalloidin. Day 14 images showed a uniform cytoskeleton network interconnecting the microsphere scaffolds in both P-15 MS and MS (Figure 7B2, C2). On day 21, the cytoskeleton arrangement in MS was lost (Figure 7B3). However, a uniform cytoskeleton arrangement was still maintained in P-15 MS suggesting stronger cell attachment and formation of higher amount of stress fibres in biomimetic scaffolds which led to maintenance of actin bundles and focal contacts between cells and P-15 MS for longer time periods (Figure 7C3). In monolayer culture, uniform multilayered cells could be seen on day 7 (Figure 7A1). With time areas without cells (black areas without fluorescence) became more prominent due to detachment of cells in the form of clusters from the well bottom, as discussed earlier (Figure 7A3).

3.4.4. Protein estimation

In spite of much higher cell counts, the matrix protein production was significantly lower than on 2D monolayer culture when compared to P-15 MS on day 1, 14 and 28. P-15 MS also showed significantly higher matrix protein production than MS at all time points (Figure 8). The results emphasize the importance of biomimetic 3D scaffolds in providing a highly favourable environment for successful tissue engineering. Although monolayer culture was able to support cell proliferation, it lacked ability to generate a supportive, protein-rich matrix.

3.4.5. Cell differentiation studies

Kinetic determination of ALP activity was performed on day 21 by determination of average change in absorbance per min of p-nitrophenyl phosphate substrate in presence of the cell

lysate. The relative ALP activity of P-15 MS was significantly higher (24 times) than 2D monolayer culture ($P < 0.05$) (Figure 9A). MS showed around 3 times higher ALP activity with respect to 2D monolayer culture, however the difference in ALP activity was not statistically significant.

OPN content was found to be significantly higher in both MS and P-15 MS in comparison to 2D monolayer culture. In case of P-15 MS, OPN content was around 22-fold higher than 2D monolayer culture. This was 2.6 fold in biomimetic P-15 MS than MS ($P < 0.05$) (Figure 9B).

Alizarin red staining showed minimal mineralization in monolayer culture. Cellular clusters which were on the verge of detaching from well bottom showed some signs of mineralization on day 21 in 2D culture (Figure 10A3). On the contrary, 3D culture systems showed formation of mineralized matrix at an early stage. P-15 MS showed a strong red coloration indicating higher mineralization than MS (Figure 10C3).

During Immunohistochemistry studies for collagen expression (28th day), cell clusters were washed off after the antigen retrieval step in case of monolayer culture due to poor phenotypic characteristics and weak cellular attachment at the well bottom. Cellular attachment was however maintained, on 3D microsphere scaffolds in both MS and P-15 MS. Collagen Type-I expression was much higher in P-15 MS in comparison to MS (Figure 11B).

4. Discussion

This study aimed to evaluate the potential of P-15 modified biomimetic PLGA microsphere scaffolds as injectable bone filler. A size of around 100 μm was selected while fabricating the microsphere scaffolds as it was expected to provide an optimum balance between the requirement to maximize the cell surface to volume ratio and the ability of each micro-carrier to support sufficient cell growth beyond the initial seeding while maintaining the injectability. To induce biomimetism, the surface of hydrophobic PLGA microspheres was modified with P-15 peptide, $^{766}\text{GTPGPQGIAGQRGVV}^{780}$, a synthetic analogue of the cell binding domain of $\alpha(\text{I})$ chain of collagen type-I, on account of previous reports indicating a key role of P-15 in osteogenesis and ultimately bone regeneration [28, 29]. P-15 is responsible for generating appropriate biomimetic environment for enhanced viable cell attachment, cell bonding and the initiation of a cascade of events (migration, alignment, proliferation and differentiation) that are necessary for optimal bone formation [27, 30-32]. It increases Type-I collagen, alkaline phosphatase and BMP-2 gene expression thus stimulating osteoblastic activity and synergising the effects of osteogenic factors to induce osteoblastic differentiation [28]. Clinically, an anorganic bovine-derived hydroxyapatite matrix/cell-binding peptide (ABM/P-15) has been found to significantly improve the outcomes of regeneration of infrabony periodontal defects following treatment when compared to open flap debridement [33].

It is reported that surfaces with textures such as nodes, pores, or random patterns are often associated with marked changes of cell morphology, cell activities, and production of regulatory factors when compared to smooth surfaces [3]. The effect of P-15 modification on the surface topography and hydrophilicity of scaffold was assessed and it was found that P-15 peptide conjugation led to an increase in surface hydrophilicity as well as nano-level roughness. Y. Wan *et al* reported enhanced cell adhesion strength due to the nano-scale or micro-scale roughness, when compared with a controlled smooth surface [4]. The width and the depth of a surface topographical structure can also influence the cell responses, since cells can orient themselves along the groove and ridge, the phenomenon commonly referred as “contact guidance” [23, 24]. Reports suggest that the alterations in adhesion structures due to the surface topography may be responsible for differences in cell signalling, which lead to changes in the cellular function like mineralization [34]. It was expected that the changes in scaffold topography due to P-15 modification could possibly have marked effects on the cellular response of the scaffold.

The synchronization between polymer degradation and replacement by natural tissue produced from cells is considered to be essential for the success of any tissue engineered scaffold [35]. Thus, *in vitro* degradation studies were performed to have an idea about the degradation characteristics which may affect biological cellular processes including cell viability, growth, tissue regeneration, and host response [36]. During degradation, scaffolds underwent hydration, swelled and later showed visible signs of bulk degradation along with generation of soluble, acidic degradation by-products resulting in acidification of external medium. However, during cell culture evaluation, hydration and swelling was visible much earlier (around 7 days) due to an added effect of enzymatic degradation in cellular environment. Thus, it is imperative to consider the effect of biological environment on the scaffold degradation while choosing a polymer for a specific tissue engineering application. Suitable measures may also be required to minimize the effect of microenvironment pH acidification due to polymer degradation. During cell culture evaluation, the polymer showed faster degradation and the degrading polymer was replaced by growing cells and ECM.

The ability of cells to adhere to the scaffold, leading to production and organization of ECM is also a central and key step to successful tissue engineering. It was observed that P-15 MS showed enhanced cell-binding capacity due to its biomimetic nature which resulted in significantly higher viable cell attachment in comparison to MS. The improved hydrophilicity and nano-level roughness generated due to P-15 surface modification probably also contributed to the improved cell attachment. Cell proliferation was analyzed until 28 days and it was found that viable cell count increased until 14 days, but was significantly reduced up to the 28th day. Biomimetic scaffolds showed a higher cell proliferation till 21 days in comparison to unmodified microspheres. After this time period, factors such as nutrient diffusion and hypoxia probably became limiting for cell growth and survival, thereby overshadowing the biomimetic effect of P-15. Acidification of the microenvironment pH due to by-products generated during polymer degradation also contributed to decreased cell viability. On day 21, a uniform layer of microsphere scaffolds interconnected with intercellular bridges could be observed in P-15 MS. Contraction due to force transfer through biomimetic environment provided by P-15 resulted in microsphere clustering, 3D colony formation and ordering of cells thus initiating physiological processes leading to cell sheet formation. This observation could be attributed to the fact that P-15 MS behaved as a collagen surrogate matrix (CSM), and were able to mimic the physiological interactions of collagen with cells, thereby leading to haptotactic cell migration, activation of signalling

pathways, induction of growth factors, cell differentiation, tissue remodelling and morphogenesis [37].

Deposition of bone in physiological conditions involves timed secretion, deposition and removal of a complex array of ECM proteins which appear in a defined temporal and spatial sequence [38]. Hence, matrix protein production is an essential component for healthy bone tissue formation. Abundant matrix protein formation, which is considered as a benchmark for successful tissue-construct formation, contributed in generation of uniform 3D colonies by holding the separate microspheres together, provided a uniform sheet-like arrangement to the scaffold-cell constructs and helped in maintaining the cellular arrangement on P-15 MS scaffolds during the long term studies. Optical microscopy and SEM studies corroborated the aforementioned observations. Biomimetic modification could further contribute to maintain the cytoskeleton arrangement for longer time periods *in vitro*. In spite of higher cell count in 2D plate, protein content was found to be much less, suggesting that cell phenotype, extracellular matrix and cytoskeleton arrangement could not be maintained in monolayer culture for longer time periods. Instead, cells were washed off during the processing due to weak attachment to the plate surface.

The formation of a collagenous matrix with mineralization is a prerequisite for a good bone repair process as mineralization plays a role in dictating and spatially orienting the deposition of ECM. The composition of the extracellular framework is dominated by a class of molecules known as collagens, each with unique features suited for its function and location. Ninety percent of the organic matrix of bone is made up by collagen Type-I, and ten percent by a variety of non-collagenous proteins [38]. Biomimetic microspheres developed significantly higher levels of mineralized ECM and showed enhanced collagen Type-I expression. High ALP activity and OPN production, even in the absence of an osteogenic medium, indicated the osteoinductive nature of P-15 and its ability to modulate cell differentiation and morphogenesis, thus supporting its possible role in skeletal reconstruction.

These results suggest the fact that P-15 modified osteoconductive PLGA microsphere scaffolds encompass the biocompatibility, mechanical strength and biodegradability of PLGA, along with the cell adhesive, proliferative and differentiative properties of osteoinductive P-15, and also eliminate the limitations of monolayer culture due to the 3D biomimetic environment provided for cell growth. In the case of 2D monolayer culture,

though a higher cell count is obtained, it was overshadowed by the weak cell attachment, poor phenotypic characteristics, low mineralization levels and cell death in the later time points.

5. Conclusions

The present study substantiates the importance of biomimetic 3D scaffolds for providing and maintaining a natural environment conducive for successful tissue regeneration and also correlates the degradation behaviour of polymeric scaffolds to cell survival. P-15 modified microsphere scaffolds showed a significantly higher cell attachment, proliferation and ECM formation, with enhanced mineralization and collagen Type-I expression, when compared to unmodified scaffolds. The results demonstrate the suitability of P-15 modified PLGA microspheres as a potential injectable scaffold for non-invasive bone tissue engineering applications.

Acknowledgements

Authors are thankful to Professor Rajendra S. Bhatnagar, Chief scientist and CEO, ENTAM, LLC, USA for providing the financial support to carry-out the research work and to Professor P. Ramarao (Director, NIPER) for allowing the use of SEM, AFM and CLSM at Centre for Pharmaceutical Nanotechnology. Technical support for microscopic techniques from Mr. Dinesh and Dr. Vijender Beniwal is duly acknowledged.

References

- [1] C. Sanchez, H. Arribart, M. M. Guille, *Nat. Mater.* 4 (2005) 277-288.
- [2] A. B. Sanghvi, K. P. Miller, A. M. Belcher, C. E. Schmidt, *Nat. Mater.* 4 (2005) 496-502.
- [3] R. G. Flemming, C. J. Murphy, G. A. Abrams, S. L. Goodman, P. F. Nealey, *Biomaterials* 20 (1999) 573-588.
- [4] Y. Wan, Y. Wang, Z. Liu, X. Qu, B. Han, J. Bei, S. Wang, *Biomaterials* 26 (2005) 4453-4459.
- [5] B. C. Tai, C. Du, S. Gao, A. C. Wan, J. Y. Ying, *Biomaterials* 31 (2009) 48-57.
- [6] M. Pegueroles, C. Aparicio, M. Bosio, E. Engel, F. J. Gil, J. A. Planell, G. Altankov, *Acta Biomater.* (2009).
- [7] R. F. Neiva, Y.-P. Tsao, R. Eber, J. Shotwell, E. Billy, H.-L. Wang, *J. Periodontol.* 79 (2008) 291-299.
- [8] A. Andukuri, W. P. Minor, M. Kushwaha, J. M. Anderson, H. W. Jun, *Nanomed.* (2009) In Press.
- [9] C. Milburn, J. Chen, Y. Cao, G. M. Oparinde, M. O. Adeoye, A. Beye, W. O. Soboyejo, *Mater. Sci. Eng: C* 29 (2009) 306-314.
- [10] H. Shin, S. Jo, A. G. Mikos, *Biomaterials* 24 (2003) 4353-4364.
- [11] N. R. Mercier, H. R. Costantino, M. A. Tracy, L. J. Bonassar, *Biomaterials* 26 (2005) 1945-1952.
- [12] K. D. Newman, M. W. McBurney, *Biomaterials* 25 (2004) 5763-5771.
- [13] B. P. Chan, T. Y. Hui, C. W. Yeung, J. Li, I. Mo, G. C. F. Chan, *Biomaterials* 28 (2007) 4652-4666.
- [14] Y. Senuma, S. Franceschin, J. G. Hilborn, P. Tissie`res, I. Bisson, P. Frey, *Biomaterials* 21 (2000) 1135-1144.
- [15] M. Borden, S. F. El-Amin, M. Attawia, C. T. Laurencin, *Biomaterials* 24 (2003) 597-609.
- [16] K. Garkhal, S. Verma, K. Tikoo, N. Kumar, *J. Biomed. Mater. Res. A* 82 (2007) 747-756.
- [17] S. W. Kang, S. W. Seo, C. Y. Choi, B. S. Kim, *Tissue Eng.* 14 (2008) 25-34.
- [18] J. M. Melero-Martin, M. A. Dowling, M. Smith, M. Al-Rubeai, *Biomaterials* 27 (2006) 2970-2979.
- [19] F. Gabler, S. Frauenschuh, J. Ringe, C. Brochhausen, P. Gotz, C. J. Kirkpatrick, M. Sittinger, H. Schubert, R. Zehbe, *Biomol. Eng.* 24 (2007) 515-520.
- [20] R. C. Mehta, B. C. Thanoo, P. P. Deluca, *J. Control. Rel.* 41 (1996) 249-257.
- [21] D. Lochmann, S. Stadlhofer, J. Weyermann, A. Zimmer, *Int. J. Pharm.* 283 (2004) 11-17.
- [22] Y. Zhu, K. S. Chian, M. B. Chan-Park, P. S. Mhaisalkar, B. D. Ratner, *Biomaterials* 27 (2006) 68-78.
- [23] Y. Wan, X. Qu, J. Lu, C. Zhu, L. Wan, J. Yang, J. Bei, S. Wang, *Biomaterials* 25 (2004) 4777-4783.
- [24] P. T. Ohara, R. C. Buck, *Exp. Cell Res.* 121 (1979) 235-249.
- [25] M. Sandor, D. Ensore, P. Weston, E. Mathiowitz, *J. Control. Rel.* 76 (2001) 297-311.

- [26] J. Panyam, M. M. Dali, S. K. Sahoo, W. Ma, S. S. Chakravarthi, G. L. Amidon, R. J. Levy, V. Labhasetwar, *J. Control. Rel.* 92 (2003) 173-187.
- [27] T. Hanks, B. L. Atkinson, *Biomaterials* 25 (2004) 4831-4836.
- [28] X. B. Yang, R. S. Bhatnagar, S. Li, R. O. Oreffo, *Tissue Eng.* 10 (2004) 1148-1159.
- [29] A. H. Valentin, J. Weber, *Keio. J. Med.* 53 (2004) 166-171.
- [30] J. J. Qian, R. S. Bhatnagar, *J. Biomed. Mater. Res.* 31 (1996) 545-554.
- [31] H. Nguyen, J. J. Qian, R. S. Bhatnagar, S. Li, *Biochem. Biophys. Res. Commun.* 311 (2003) 179-186.
- [32] A. Palmieri, F. Pezzetti, G. Brunelli, I. Zollino, L. Scapoli, M. Martinelli, M. Arlotti, F. Carinci, *J. Biomed. Sci.* 14 (2007) 777-782.
- [33] A. Kasaj, B. Rohrig, C. Reichert, B. Willershausen, *Clin. Oral Investig.* 5 (2008) 5.
- [34] B. Nebe, F. Lüthen, R. Lange, P. Becker, U. Beck, J. Rychly, *Mater. Sci. Eng: C* 24 (2004) 619-624.
- [35] H. J. Sung, C. Meredith, C. Johnson, Z. S. Galis, *Biomaterials* 25 (2004) 5735-5742.
- [36] J. E. Babense, J. M. Anderson, L. V. McIntire, A. G. Mikos, *Adv. Drug Deliv. Rev.* 33 (1998) 111-139.
- [37] R. Bhatnagar, S. Li, *Conf. Proc. IEEE Eng. Med. Biol. Soc.* 7 (2004) 5021-5023.
- [38] M. Riminucci, P. Bianco, *Brazilian J. Med. Biol. Res.* 36 (2003) 1027-1036.

Figure legends:

Figure 1. AFM topographies for (A) MS, and (B) P-15 MS

The Ra value and vertical axis scale was 5.33 ± 0.45 nm and 300 nm for PLGA MS; and 200.20 ± 13.37 nm and 3 μ m, for P-15 PLGA MS, respectively

Figure 2. Degradation study parameters and scanning electron micrographs of MS showing sequential events during degradation* A) Weight average molecular weight (M_w) loss[@] and weight loss; B) Degree of hydration and change in medium pH; Morphological changes at (C) 0 h, (D) 15 days, (E) 27 days and (F) 42 days at 100x magnification. Insets correspond to 500x magnification of respective images

*Study was performed in phosphate buffer (0.1 M, pH 7.4) at 37°C and 100 rpm, without media replacement (n=4) @ As determined by GPC

Figure 3. Cell adhesion on MS, P-15 MS and 2D monolayer culture after 24h of cell seeding

$P^* < 0.050$ Vs 2D, $P\# < 0.050$ Vs MS, n=3 (One way ANOVA followed by Student-Newman-Keuls test)

Figure 4. Cell viability and proliferation on MS, P-15 MS (A) and 2D monolayer culture (B), during *in vitro* cell culture study

Initial MG-63 cell seeding: 0.2 million/well in MS and P-15 MS; 40000 per well in 2-D plate. $P^* < 0.050$ Vs MS at day 1 and day 7, $P\# < 0.001$ Vs day 1 and day 28 for both MS and P-15 MS, $P@ < 0.001$ Vs day 1 and day 21 for P-15 MS, $P^{\wedge} < 0.001$ Vs day 28 for P-15 MS, $P\% < 0.050$ Vs day 21 and day 28 for P-15 MS, $P < 0.001$ Vs day 1, day 7 and day 28 for 2D, $P\blacklozenge < 0.001$ Vs day 21 for 2D, $P\bar{V} < 0.001$ Vs day 1 and day 28 for 2D. Error bars represent mean \pm SD, n=3. (One way ANOVA followed by Student-Newman-Keuls test)

Figure 5. Microscopic observation of 2D plate (A), MS (B) and P-15 MS (C) scaffolds after day 1 (1), day 7 (2), day 14 (3), day 21 (4) and day 28 (5) of *in vitro* cell culture studies

Figure 6. Scanning electron micrographs of MS (A) and P-15 MS (B) samples after 7 days of cell culture (1000x magnification)

Figure 7. Cytoskeletal actin distribution and organization of MG-63 cells grown on 2-D plate (A), MS (B) and P-15 MS (C), after day 7 (1), day 14 (2) and day 21 (3) of *in vitro* cell culture. Dotted circle represents microsphere perimeter

Figure 8. Extracellular matrix production as determined by Bradford assay during *in vitro* cell culture studies for 2D plate, MS and P-15 MS

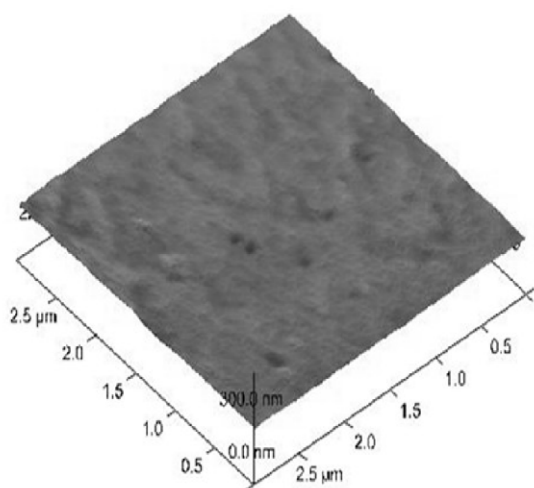
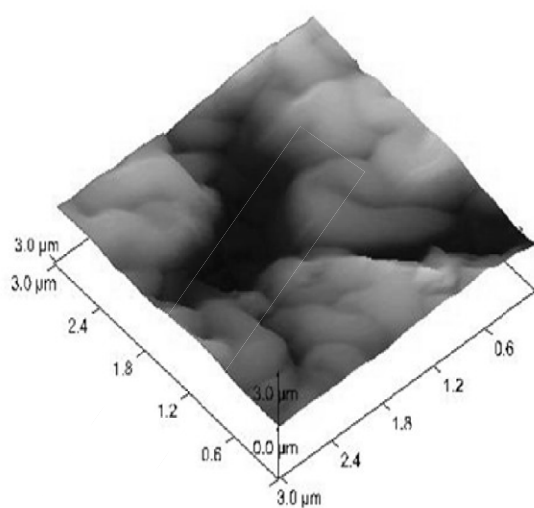
$P^* < 0.050$ Vs 2D and MS at day 1, $P^{**} < 0.050$ Vs 2D and P-15 MS at day 7, $P^{***} < 0.050$ Vs 2D and MS at day 14, $P^{****} < 0.050$ Vs 2D and MS at day 28, $P^{\#} < 0.050$ Vs day 1, day 7 and day 28 for both 2D and MS, $P^{\#\#} < 0.001$ Vs day 1, day 7 and day 28 for P-15 MS, $P^{\#\#\#} < 0.050$ Vs day 1 and day 28 for 2D. Error bars represent mean \pm SD, $n=3$. (One way ANOVA followed by Student-Newman-Keuls test)

Figure 9. Relative Alkaline phosphatase (ALP) activity and osteopontin (OPN) content of MG-63 cells on 2D monolayer culture, MS and P-15 MS after 21 days of *in vitro* cell culture

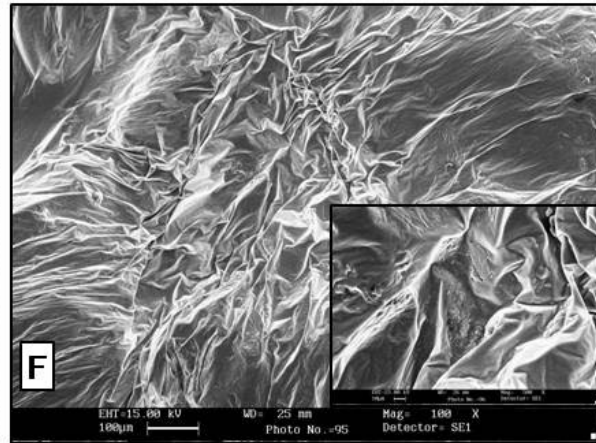
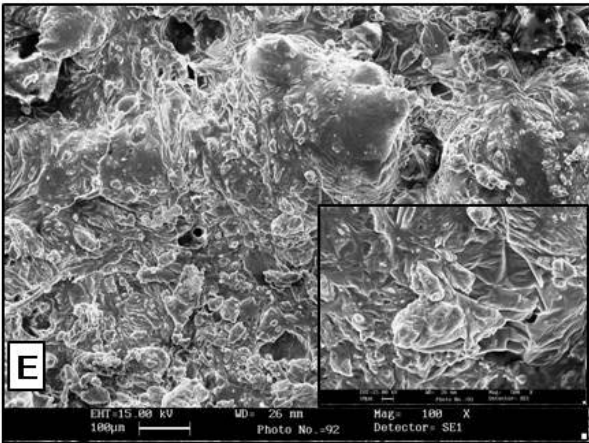
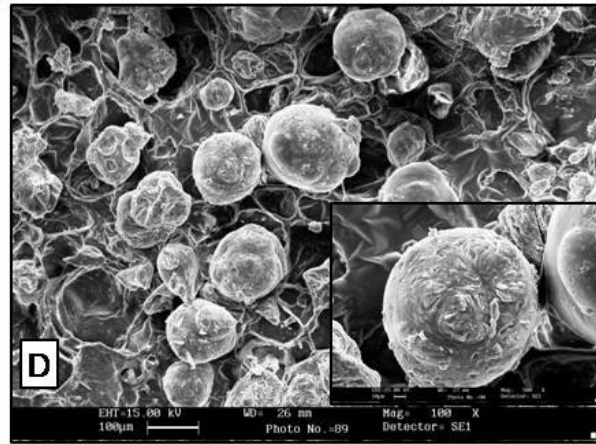
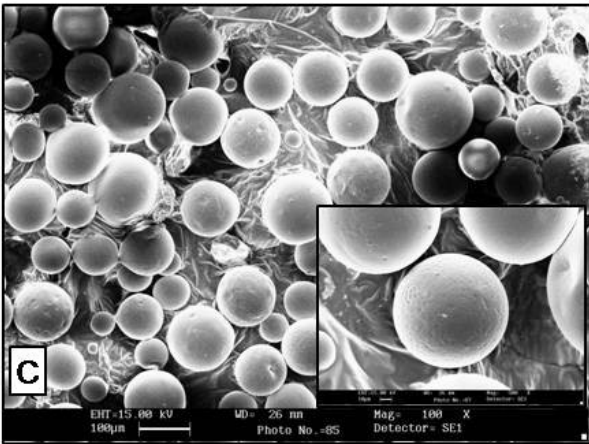
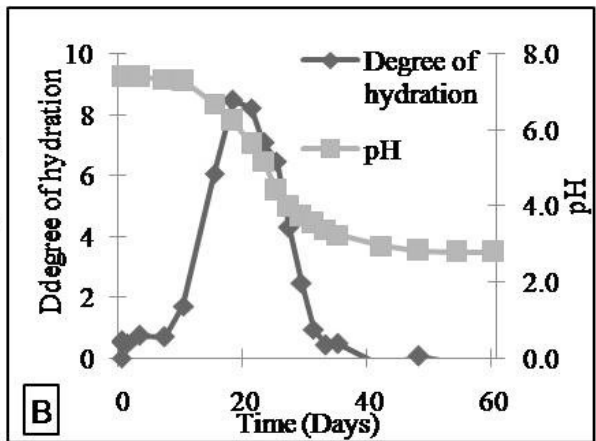
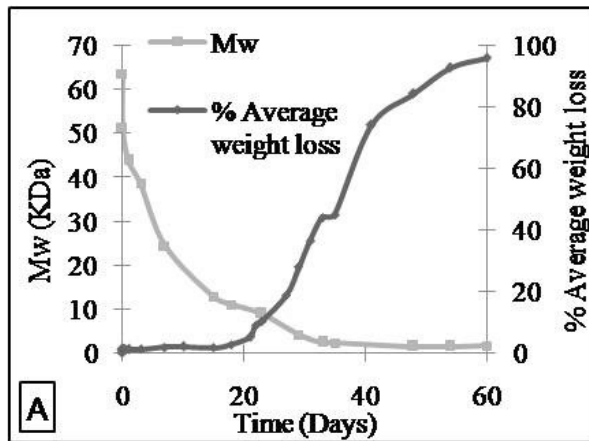
ALP production is presented relative to ALP activity by 2D monolayer culture. $P^* < 0.050$ Vs 2D, $P^{\#} < 0.050$ Vs MS, (One way ANOVA followed by Student-Newman-Keuls test), $n=3$

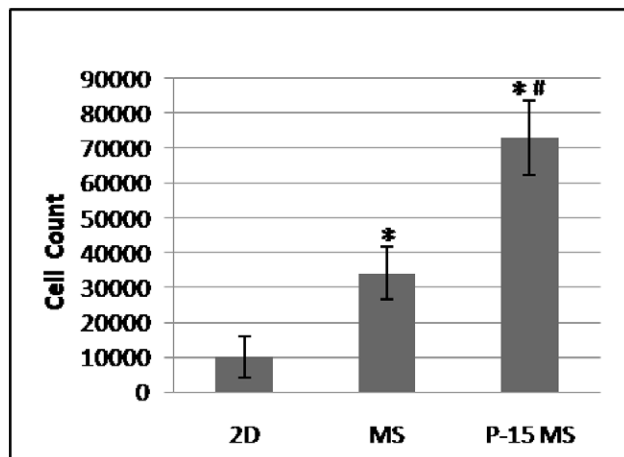
Figure 10. Mineralization of extracellular matrix in 2D (A), MS (B) and P-15 MS (C) scaffolds after day 7(1), day 14 (2) and day 21 (3) of *in vitro* cell culture indicated by alizarin red staining

Figure 11. Immunohistochemistry of Type I Collagen on MS (A) and P-15 MS (B), after 28 days of cell culture

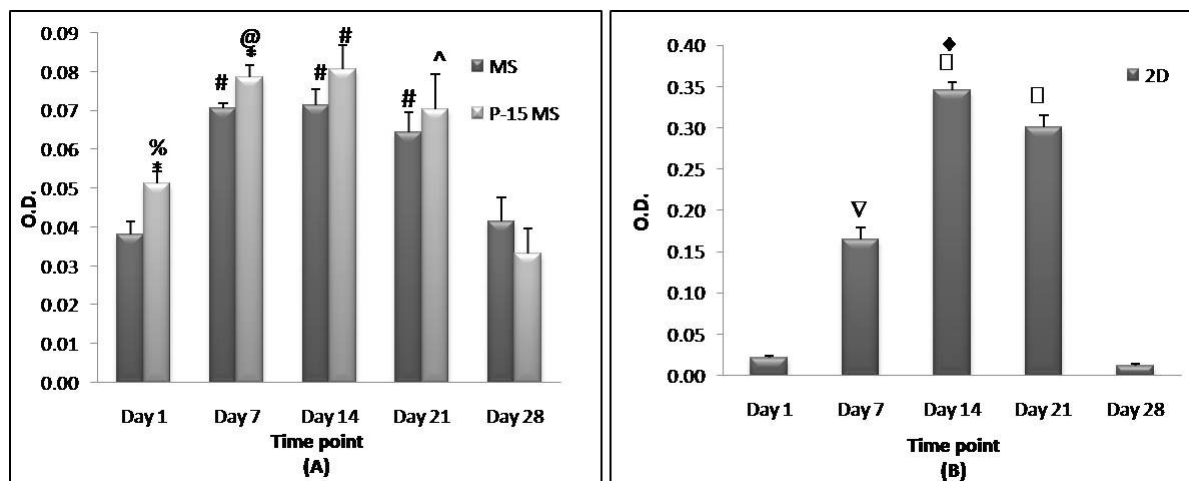
**A) MS****B) P-15 MS**

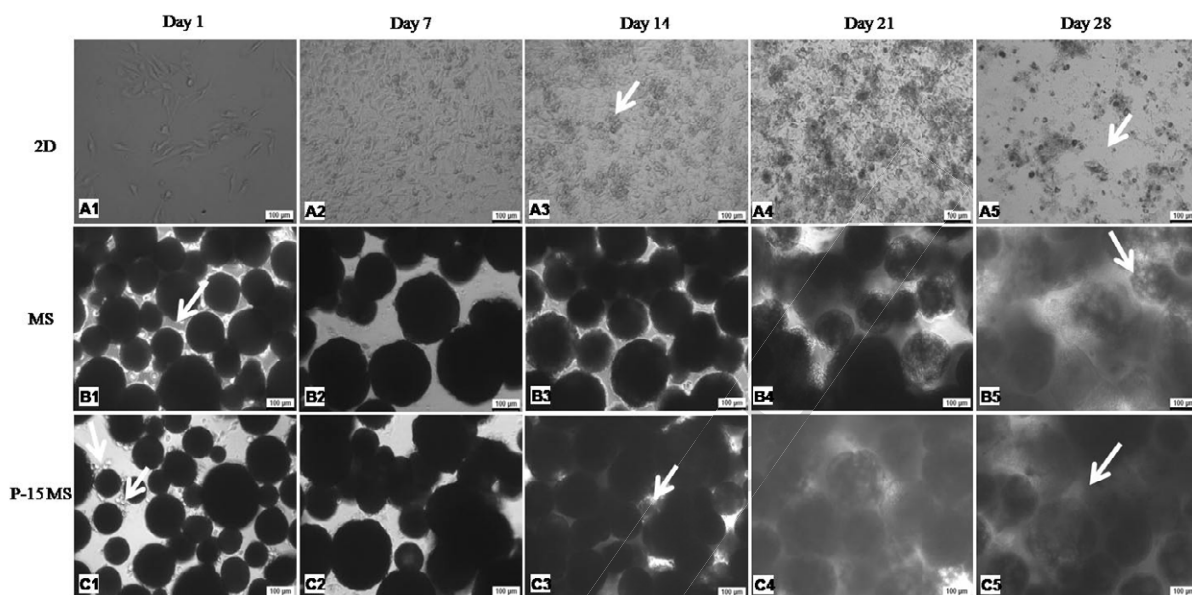
ACCEPTED MANUSCRIPT

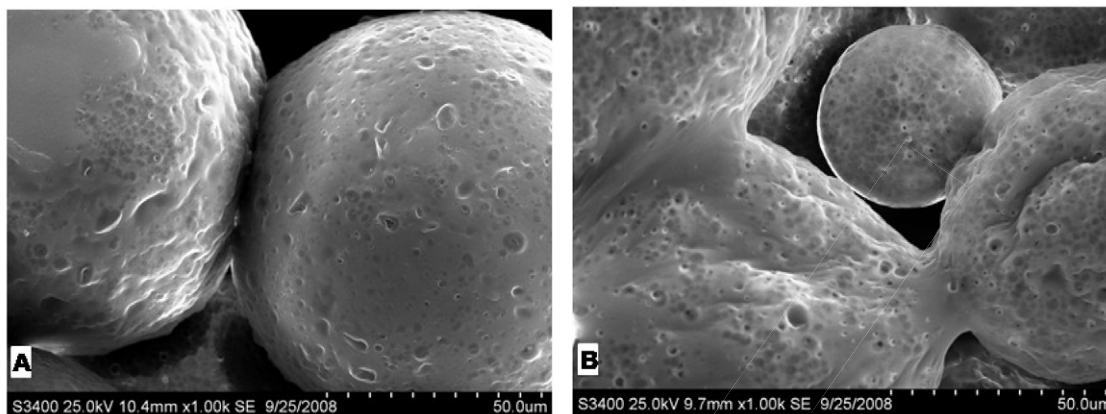




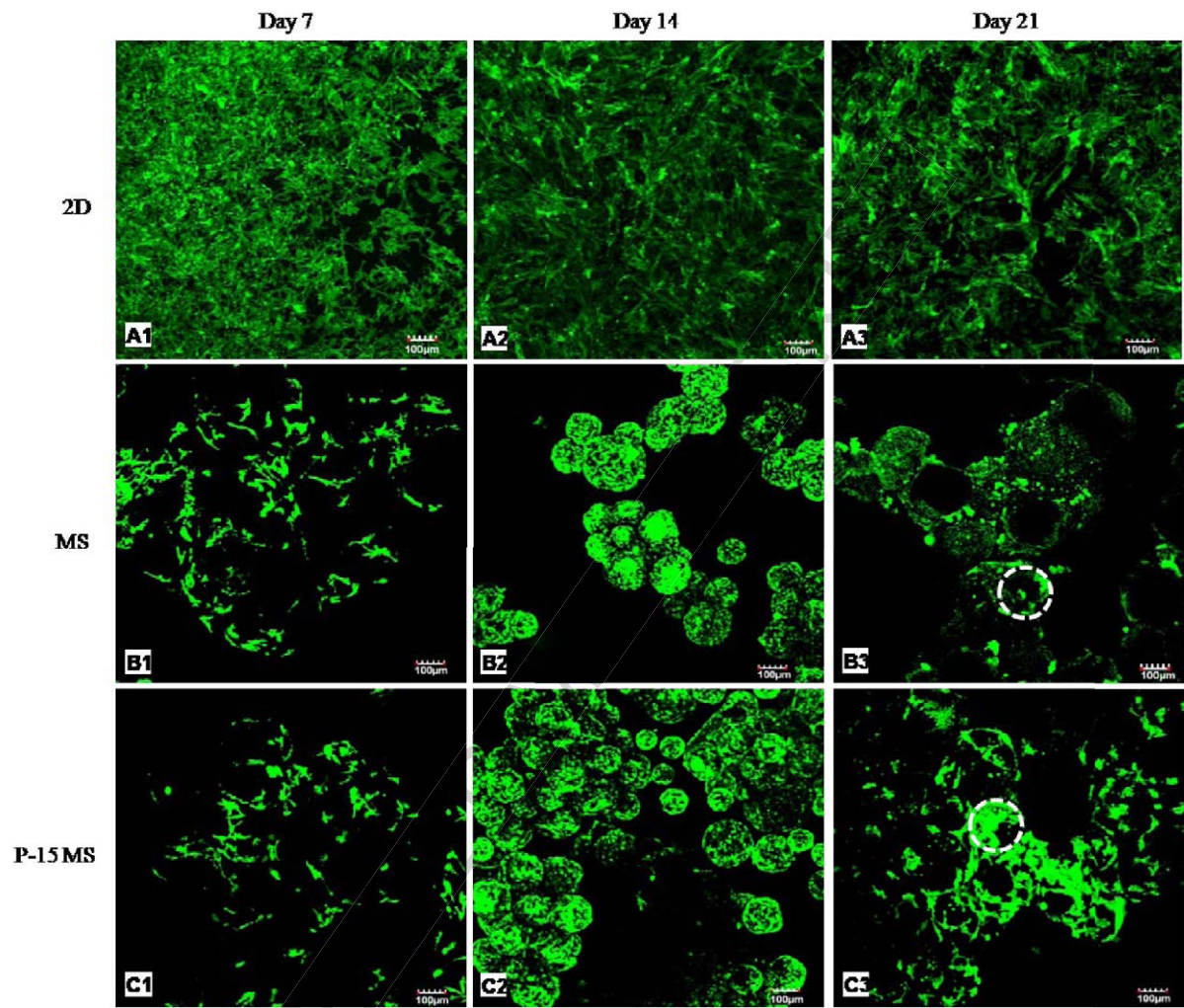
ACCEPTED MANUSCRIPT

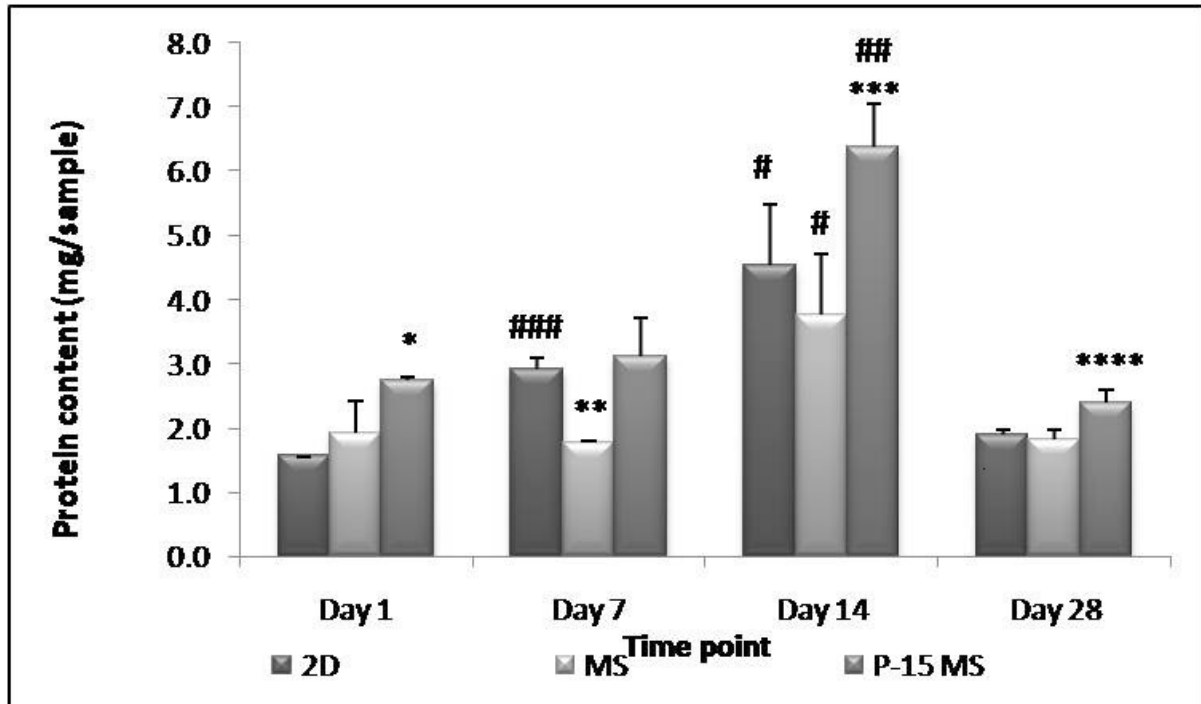




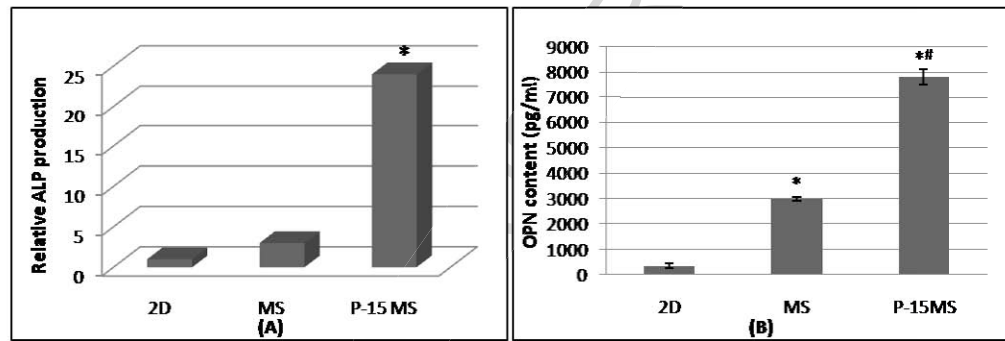


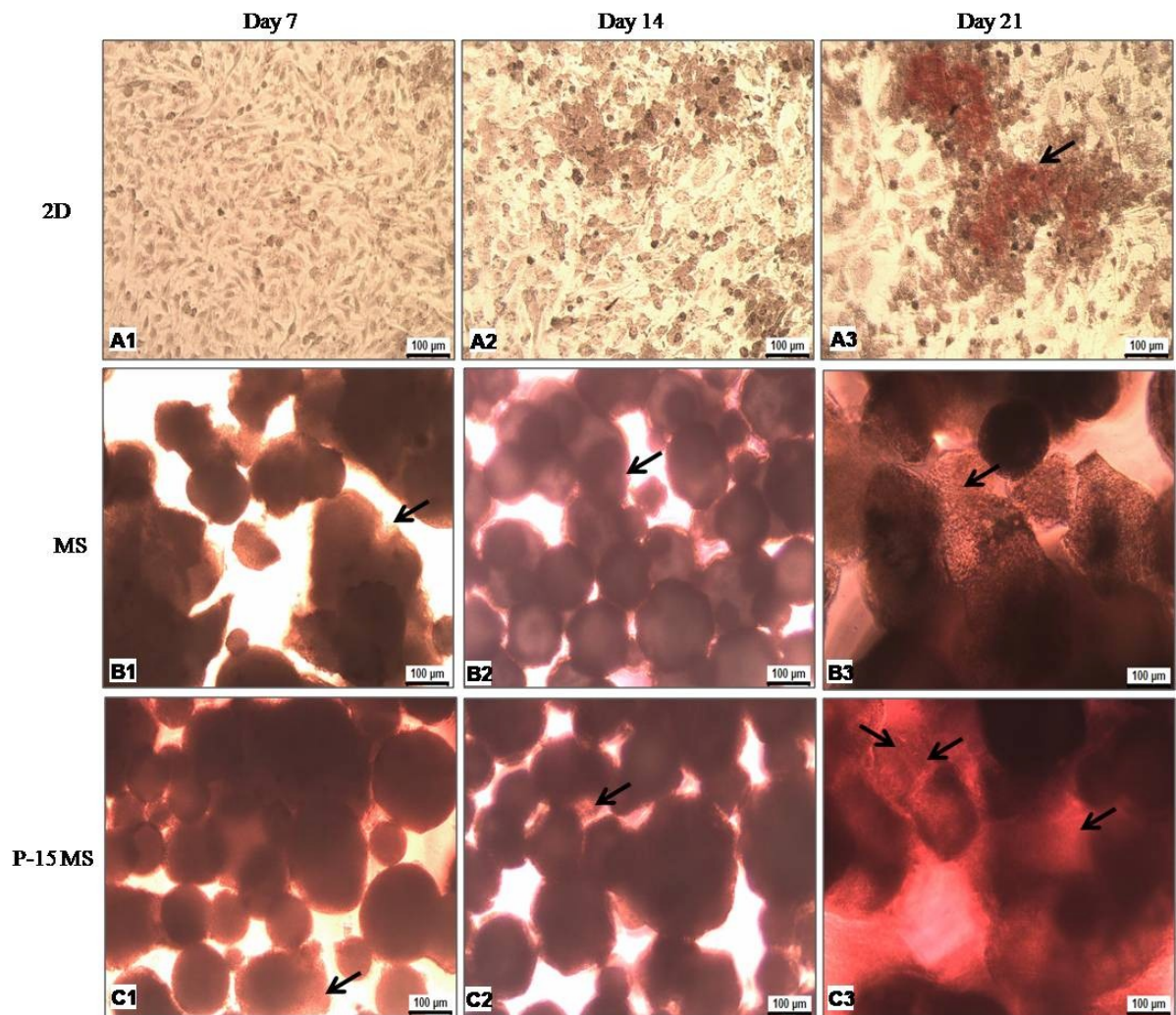
ACCEPTED MANUSCRIPT

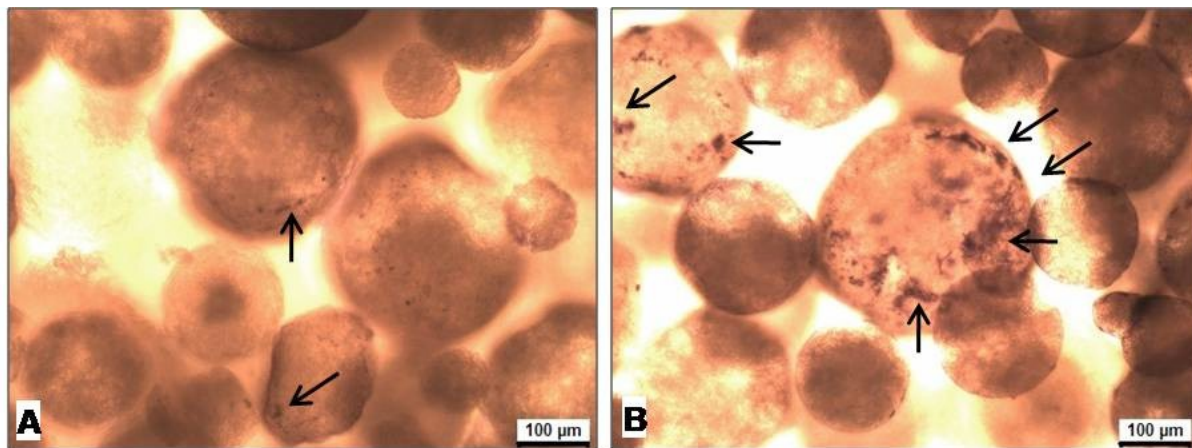




ACCEPTED MANUSCRIPT







ACCEPTED MANUSCRIPT